Nanoscale

Accepted Manuscript

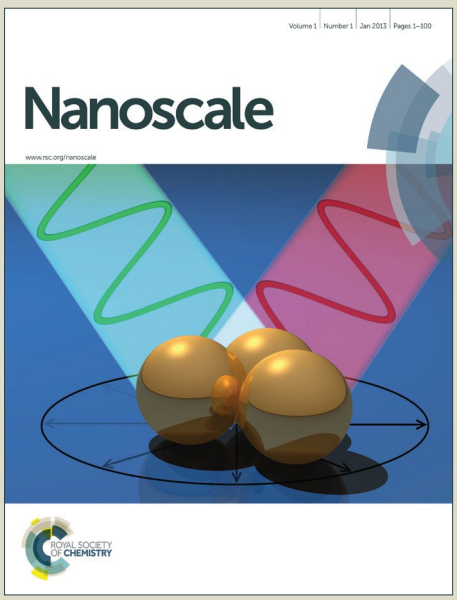

ROYAL SOCIETY OF CHEMISTRY

www.rsc.org/nanoscale

Cite this: DOI: 10.1039/c0xx00000x

www.rsc.org/xxxxxx

ARTICLE TYPE

Curcumin Modified Silver Nanoparticles for Highly Efficient Inhibition of Respiratory Syncytial Virus Infection

Xiao Xi Yang, Chum Mei Li and Cheng Zhi Huang*

Received (in XXX, XXX) Xth XXXXXXXXX 20XX, Accepted Xth XXXXXXXXX 20XX

DOI: 10.1039/b000000x

Interactions between nanoparticles and viruses have attracted increasing attention due to the antiviral activity of nanoparticles and the resulting possibility to be employed as biomedical interventions. In this contribution, we developed a very simple route to prepare uniform and stable silver nanoparticles (AgNPs) with antiviral properties by using curcumin, which is a member of the ginger family isolated from rhizomes of the perennial herb curcuma longa and has a wide range of biological activities like antioxidant, antifungal, antibacterial and anti-inflammatory effects, and acts as reducing and capping agents in this synthetic route. Tissue culture infectious doses ($TCID_{50}$) assay showed that the curcumin modified silver nanoparticles (cAgNPs) have highly efficient inhibition effect against respiratory syncytial virus (RSV) infection, giving a decrease of viral titers about two orders of magnitude at the concentration of cAgNPs under which no toxicity was found to the host cells. Mechanism investigations showed that cAgNPs could prevent RSV from infecting the host cells by inactivating the virus directly, indicating that cAgNPs are a novel promising efficient virucide for RSV.

Introduction

The use of nanomaterials in medicine raises high expectation for human health and is already contributing to the development of new drugs, biologics, and medical devices, indicating that developing nanoparticle-based drug delivery, biomolecular sensing, biological imaging and nanoparticle-based therapies shows high promise.[1, 2] The point we are concerned about is the suppressive effect of nanoparticles on virus infecion.[3-11] In the majority of researches, the antiviral effect is achieved by preparing nanoparticles modified by different functional biomolecular covers, wherein the modified covers can inactivate the virus directly or make the recognition of the receptors on the host cells surface and block viral entry into cells. Functional gold nanoparticles,[3-7] ZnO nanoparticles,[8] carbon nanomaterials,[9] nanoclay[10] and silicon nanoparticles[11] have been reported to display antiviral properties to some extent. It seemed that the use of metal nanoparticles provides a potential opportunity for novel antiviral therapies. Since metal nanoparticles had a broad-spectrum antiviral ability and are not prone to inducing resistance.[12]

Among the noble-metal nanomaterials, silver nanoparticles (AgNPs) have received considerable attention owing to their attractive antibacterial,[13] antifungal, and antiviral properties. In vitro studies have demonstrated that AgNPs could be used as antiviral agents against the human immunodeficiency virus (HIV),[14-16] H1N1 influenza A virus,[17,18] monkeypox virus,[19] adenovirus,[20] Tacaribe virus,[21] hepatitis B virus (HBV), Herpes simplex virus (HSV)[22, 23] and so on. It has suggested that silver nanoparticles bind with viral envelope glycoprotein and inhibit the virus by binding to the disulfide bond regions of the cluster of differentiation 4 (CD4) binding domain within the HIV-1 viral envelope glycoprotein gp120.[14,15] Moreover, AgNPs have high binding affinity with the double-stranded of HBV, and thus different sized AgNPs can inhibit the production of HBV RNA and extracellular virions.[24] Because of their multiple interactions with glycoprotein receptor and viral envelope glycoprotein, AgNPs can inhibit the viral multiplication inside the host cell by preventing the replication or blocking the entry of virus particles inside the host cell, and thus have strong antiviral potential.[12] In case of cytotoxicity, nanoparticles with large sizes showed higher level of cytotoxicity than those with small sizes. Furthermore, it has reported that smaller the size more interaction and more inhibition take place. Because the small size of nanoparticles have large surface areas, which can result in a direct interaction with viral envelope proteins. Moreover, the small nanoparticles can enter into the host cell easily and interact with the viral genome to interfering the viral replication.[25]

Curcumin, [1,7-bis(4 hydroxy-3-methoxy phenyl)-1,6 heptadiene-3,5-diene], a member of the ginger family and is isolated from rhizomes of the perennial herb curcuma longa.[26,27] As natural polyphenols, curcumin has various functions including antioxidant, antifungal, antibacterial, anti-inflammatory, antiviral effects and so on.[28,29] Recently, Kojima's group reported that curcumin could prevent replication and budding of respiratory syncytial virus (RSV). The detail mechanism had been studied at the genetic levels thoroughly and their research has a profound

significance.[30] However, the poor solubility in water and low bioavailability of curcumin greatly confine its applicable range in clinics.[31]

RSV, a negative-sense, single-stranded enveloped RNA virus and belongs to the paramyxoviridae family,[32-34] targets ciliated cells of the bronchial epithelium and type 1 pneumocytes in alveoli, causing acute lower respiratory infections in infants, the elderly and immunocompromised individuals.[35-37] RSV infects patients earlier in life with greater consequences than other respiratory viruses and causes more frequent and severe infections. In children, RSV can progress to bronchiolitis or pneumonia with an increased chance of significant morbidity or death, and previous infections do not lead to persistent immunity, making enhancing reinfection possibility throughout life without significant antigenic change.[34,38] Therefore, effective and specific methods for early diagnosis of RSV and effective treatments used for RSV infections are of great importance. Our group have established a series of sensitive detection methods and new labelling routes about the RSV, and have realized the real-time tracking of RSV.[39-44] Currently there have been two antibodies palivizumab (Respigam ™ and Syngis ™) approved for human beings use.[45] The two antibodies, however, are limited due to the risk of transmission of blood-borne pathogens, limited effectiveness and high cost. Meanwhile, the only antiviral drug (ribavirin) is available for treating severe RSV infection. So it is a need to develop cheap, safe and effective antivirals for RSV infection, and it has shown high promise to develop a new modality to inhibit viral infection, for example, by fabricating DNA conjugated gold nanoparticle (DNA-AuNP) networks on the host cell membranes as a protective barrier.[46] In this manuscript, we hope to develop new nanoparticles, which can interfere the interaction between RSV and the host cells, and block viral entry into cells. Considering that the excellent

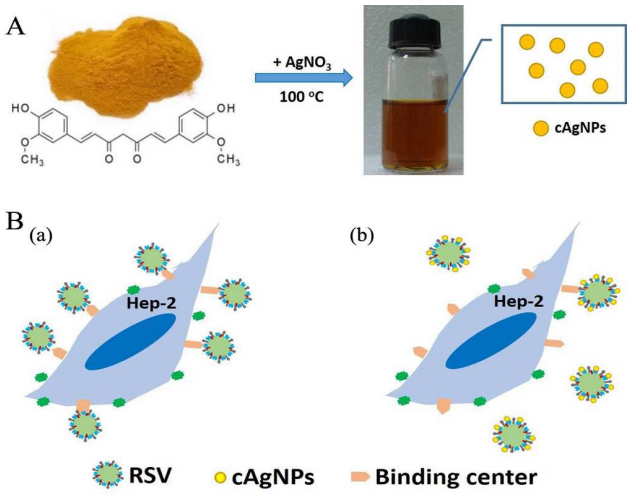

Scheme 1. Schematic representation of the synthesis of cAgNPs (A) and a proposed inhibition mode of cAgNPs against RSV infection (B). The inhibition mode of (B) shows that cAgNPs can reduce the binding ability of virus with the binding centers on the surface of cells (b) as compared to those without cAgNPs (a).

properties both of curcumin and AgNPs, and the breakage of intramolecular hydrogen bonding can increase the availability of curcumin in water at high temperature, we expected that curcumin modified AgNPs should have excellent antiviral activity against RSV infection.

Kojima's finding was very interesting and attactive,[30] and occurred to us to synthesize small, uniform, and stable mono-dispersed curcumin-AgNPs (cAgNPs), which might exert synergistic antiviral effects of curcumin and AgNPs and thus act as smart nanomedicine to RSV infection.

Experimental

Materials

Curcumin was purchased from Aladdin, while $AgNO_3$ was from Shanghai Shenbo Chemical Co., Ltd. (Shanghai, China). Dimethyl Sulphoxide (DMSO) was commercially available from Beijing Dingguo Changsheng Biotechnology Co. Ltd (Beijing, China) and used to dissolve curcumin at first. K_2CO_3 was obtained from Chengdu Kelong Chemical Co., Ltd., (Chengdu, China) to accommodate the pH of solution. Human laryngeal epithelial type 2 (Hep-2) cells was commercially obtained from XiangYa School of Medicine (Changsha, Hunan), while respiratory syncytial virus (RSV) was commercially available from Guangzhou biotest biological technology co., LTD. The Cell Counting Kit-8 (CCK-8) reagent was purchased from Dojindo (Kumanmoto, Japan). RPMI 1640 was purchased from Hyclone (USA) and the fetal bovine serum (FBS) was commercially obtained from GIBCO (USA). TRizol reagent was purchased from Life Technologies (Carlsbad, USA). The iScript™ cDNA synthesis kit and iQ™ SYBR Green Supermix were commercially available from Bio-Rad (California, USA).

Apparatus

The UV-vis absorption spectrum of cAgNPs was acquired using a Hitachi U-3100 UV-vis spectrometer (Tokyo, Japan). A Hitachi S-4800 scanning electron microscopy (SEM) and a JEM-2010 transmission electron microscopy (TEM, Tokyo, Japan) were used to identify the size and shape of cAgNPs. A Biotek Microplate Reader (USA) was used to measure the optical density (OD) of the solution at 450 nm in the cytotoxicity test. Immune- fluorescence imaging was performed with an Olympus IX81 microscope with a 60× objective (Tokyo, Japan). A Shimadzu FTIR-8400S Fourier transform infrared (FTIR) spectrophotometer (Kyoto, Japan) was employed to measure the IR spectra. Elemental analysis was performed on a Thermo ESCALAB 250 X-ray photoelectron spectrometer (USA). A Malvern dynamic light scattering (DLS) Nano-ZS zetasizer (England) was used to measure the size and ζ-potential of the cAgNPs. METTLER TGA 1/1600HT (Mettler, Swiss) was used to investigate the thermal stability of cAgNPs. The gene expression levels of cytokines were detected by a Bio-Rad iCycler Thermal Cycler w/iQ5 Optical Module for RT-PCR (California, USA).

Preparation of the cAgNPs

All glassware used was thoroughly cleaned using chromic acid before use. In a 100 mL flat-bottomed flask with a condenser, 250 μL of 20 mM curcumin dissolved in DMSO was diluted into 22.5 mL ultra-pure water, and then slightly adjusted to alkaline with K_2CO_3. With vigorous stirring at 100 °C, 2.5 mL $AgNO_3$ (10 mM) was quickly added in the mixture. The color changes from blood red to yellow brown after few minutes. By keeping vigorous stirring at 100 °C for 1 hour, the mixture was then cooled down to room temperature. The mixture was finally ultra-filtrated, and the as-prepared cAgNPs were then transferred for optical and shape characterization, and the antiviral study against RSV infection. For comparison, citric acid modified AgNPs were prepared according to the conventional method.[47]

Biocompatibility of cAgNPs in Hep-2 cells

The in vitro cellular viability of the as-prepared cAgNPs was evaluated using the CCK-8 cell viability assay. First, approximately 1.0×10^4 Hep-2 cells/well were seeded in 96-cell plates and were fed with RPMI 1640 containing 2% fetal bovine serum (FBS). After 24 hours of incubation in a humidified incubator with 5% CO_2 at 37 °C, the medium was removed from each well, and Hep-2 cells were washed with phosphate buffered saline (PBS, pH 7.4). Then, sample solutions (cAgNPs with different concentrations) or the control solutions were added in and incubated with cells for 24 h to 72 h. Each concentration was tested with 6 sets of parallel samples. After that, the culture medium was replaced with CCK-8 reagent and incubated for another 1h at 37 °C. The last step was measuring the optical density (OD) at 450 nm with a Biotek Microplate Reader. The viability of cells was expressed as the percentage of control untreated cells (100%).

Assays for antiviral activities

Hep-2 cells were plated at 8.0×10^4 cells/well in 24-well plates and incubated for 24 hours at 37 °C. To analyse how cAgNPs affect the infectivity of RSV, the virus pre-treatment assay was taken as follows. RSV were pre-incubated with series of cAgNPs at 4 °C for 1 hour, then cultured with Hep-2 cells for 2 hours at 37 °C. After that, cell monolayers were washed with PBS to remove non-adherent virus and cAgNPs, and further incubated with RPMI 1640 (containing 2% FBS) at 37 °C. The cell pret-reatment assay was performed by incubating Hep-2 cells with series of cAgNPs for 1 h, then cells were washed with PBS and infected with RSV. After the virus adsorption, the non-adherent RSV were washed away with PBS and cells were overlaid with RPMI 1640 (containing 2% FBS) at 37 °C. The cell post-treatment assay started by infecting Hep-2 cells with RSV for 2 h. Following the adsorption period, the inocula were removed, cells were washed with PBS and then incubated with series of cAgNP for 1 h at 37 °C. The cAgNPs were afterwards removed, cells were washed with PBS and overlaid with RPMI 1640 (containing 2% FBS). Negative (cells only) and positive (cells infected with RSV without nanoparticles) controls were set as well. Cytopathic effect (CPE) was observed in inoculated cells on the third day. So, the medium was discarded and washed with PBS. After that, 200 μL PBS was added per well, and the plate was freezing and thawing repeated for three times. Then, the mixture were centrifuged for 10 min at 3000 rpm to remove cell debris, and the supernatant containing RSV were collected separately and used for viral titer assay.

Viral titer assay

The viral titer assay of RSV was measured by using tissue culture infectious doses ($TCID_{50}$) test. Hep-2 cell monolayers were seeded at 1.0×10^4 cells/well in 96-well plates, 24 hours before infection. Serial 10-fold dilutions of the separately collected RSV were made in serum-free medium, and 0.3 mL was used to infect cells for 2 hours at 37 °C. Virus was aspirated from each well, and the RPMI 1640 with 2% FBS was added. The plates were incubated at 37 °C with 5% CO_2 for a week. A 50 μL volume of 2.5% glutaraldehyde and 0.05% neutral red in PBS replaced the growth medium to stain live cells. The final value of $TCID_{50}$ is calculated according to Reed-Muench formula.

Plaque assay

RSV plaque reduction assay was performed on Hep-2 cells. This assay is typically used to quantitate the infectious virus by assessing the plaque forming units (PFU). For this assay, Hep-2 cells were seeded into 24-well dishes at a concentration of 2.5×10^5 cells/well. Confluent monolayers of cells were inoculated with 200 μL of virus suspensions (multiplicity of infection (MOI) was 5, 10, 15, 20) with or without cAgNPs at 37 °C. After 2 h incubation, the non-adherent virions and cAgNPs were removed and the cells were overlaid with 1.0 mL of RPMI 1640 medium supplemented with final concentration of 2.5 % FBS and 1.5 % Agar. After incubating for a week, the cells were fixed with 2.5 % formaldehyde and stained with 0.05 % neutral red solution.

Indirect immunofluorescence assay

Inhibitory effect of the cAgNPs on RSV infection was further evaluated by immunofluorescence. Twenty-four hours before infection, Hep-2 cells (1.0×10^5 cells) were cultured in 35 mm glass-bottom cell culture dishes (NEST. Corp.). RSV, RSV pre-treated with cAgNPs at 4 °C for an hour and the mixture of RSV and cAgNPs then infected the Hep-2 cells at 37 °C for 30 minutes. The other group was that Hep-2 cells pre-incubated with cAgNPs for 1 h before RSV infection. After washing with PBS to remove non-adherent virons and cAgNPs, the cells were fixed in 4% paraformaldehyde for 30 minutes at room temperature. This step was followed by blocking with 2% bovine serum albumin for an hour at 37 °C. After blocking, the cells were incubated with primary antibody (anti-RSV G protein) incubation for 1.5 hours at 37 °C, followed by incubation with secondary antibody (Dylight 488-conjugated goat anti-mouse Ig G) for another 45 minutes at 37 °C. The last step was that cells were stained with Hoechst 33258 (1 μg/mL) for 10 minutes at room temperature. Washing three times with ice-cold PBS was made after each incubation step. Fluorescent images were acquired using an Olympus IX-81 inverted microscope equipped with an Olympus IX2-DSU confocal scanning system and a Rolera-MGi EMCCD. The image analyses were performed with Image-Pro Plus software.

Table 1. Primer pairs used in this study

Gene Name	Sequence	
	Forward	Reverse
β-actin	CGCGAGAAGATGACCCAGATC	CATGAGGTAGTCAGTCAGGTCCC
IL-1β	CCCAGAGAGTCCTGTGCTGAATG	GAGAGCTGACTGTCCTGGCTGAT
IL-6	AGCCCTGAGAAAGGAGACATG	GCAAGTCTCCTCATTGAATCCAG

Real-time PCR detection of IL-1β and IL-6 mRNA levels

Cells were harvested at 8 and 24 h after RSV infection at an MOI of 1 and the total RNA was extracted using TRizol reagent according to manufacturer's protocol. The integrity of the RNA was verified by 1% agarose electrophoresis and scanned with a gel imaging system. Then, RNA was reverse-transcribed into cDNA according to the manufacturer's recommendations of iScript™ cDNA synthesis kit. Real-time PCR detection was performed using an iQ™ SYBR Green Supermix with a Bio-Rad iQ5 real-time PCR system. The PCRs were amplified at cycling conditions of: 95 °C for 5 min and 40 cycles (30 s at 95 °C, 30 s at 60 °C and 45 s at 72 °C) in triplicate. The sequences of primer pairs are listed in Table 1. The mRNA levels of IL-1β and IL-6 were semi-quantitatively determined and normalized to the expression of housekeeping gene β–actin.

Statistical analysis

Experimental data were presented as the mean ± standard deviation (SD) of the mean. The *t*-test (Excel, Prism 5 statistical and graphing software) were used for the data analysis. $P < 0.05$ was considered to indicate a statistically significant difference.

Results and discussion

Preparation and characterization of cAgNPs

The synthesis of AgNPs in solution usually contains three main components, namely, metal precursors, reducing agents and capping agents.[48] However, reducing agents and organic solvents used in chemical reduction, such as hydration hydrazine and sodium borohydride, are highly reactive and pose potential environmental and biological risks.[49] Our method to prepare uniform AgNPs only involves in the use of curcumin and $AgNO_3$ without organic solvents, and curcumin plays roles both as reducing agent and capping agent.

The as-prepared cAgNPs were uniform and mono-dispersed, and displayed yellow blown color with a characteristic silver plasmon band at 410 nm in the UV-vis region (Figure 1a), which have the average diameter about 11.95 ± 0.23 nm (Figure 1b) analysed from SEM image by counting 220 particles (Figure 1c). High resolution transmission electron microscopy imaging showed that the lattice of the as-prepared cAgNPs is 0.23 nm and Ag atoms were mainly deposited on the {111} facets (Figure 1d). Dynamic light scattering (DLS) measurements showed that the cAgNPs have a hydrodynamic diameter of 19.72 ± 0.54 nm (Figure 1e) and a zeta-potential of -25.7 ± 0.7 mV (Figure 1f).

XPS spectra showed that the generation of zero valence state of silver in cAgNPs has occurred (Figure 2a and b). The thermogram clearly indicated a strong enhancement in the thermal stability compared to curcumin only (Figure 2c). FTIR

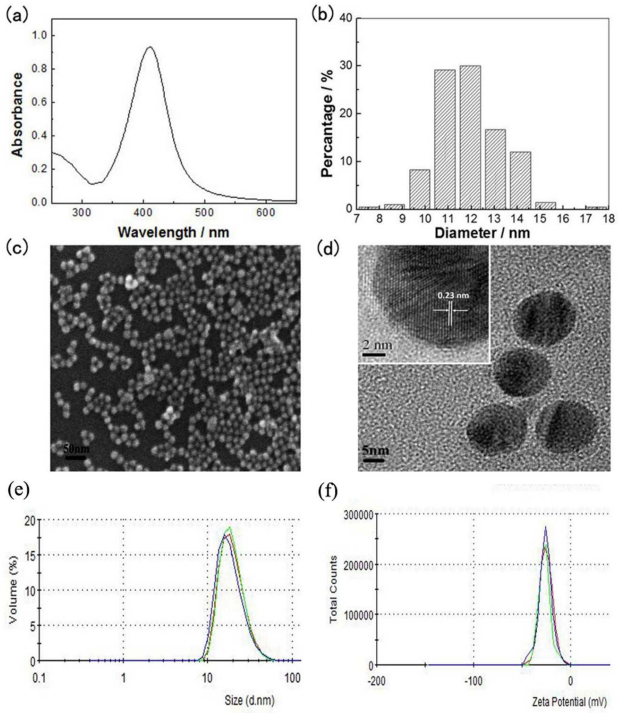

Figure 1. Characterization of cAgNPs. UV/vis absorption spectrum of the cAgNPs (a) and size distribution of the silver nanoparticles as measured by SEM analysis and calculated with 220 particles (b). SEM images (c) and representative HRTEM images of cAgNPs (d) showed the morphology of cAgNPs. The DLS data showed the size distribution (e) and the zeta-potentia (f) of cAgNPs.

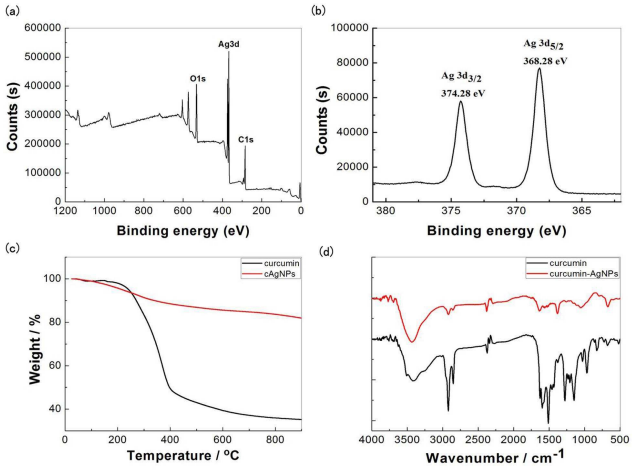

Figure 2. The XPS of as-prepared cAgNPs (a and b), TGA (c) and FTIR (d) spectrum of curcumin and cAgNPs.

spectra showed that both curcumin and cAgNPs have different functional groups, except that phenolic hydroxyl and methoxy groups (-OCH_3). As Figure 2d shows, the absorption peaks at 3240 cm^{-1}, the stretching vibration of phenolic hydroxyl groups, and 2920 cm^{-1}, the asymmetric C-H stretching of -OCH_3 groups, appear either in curcumin or cAgNPs, indicating that the synthetic reaction of cAgNPs does not involves in the phenolic hydroxyl and the methoxy groups. Since the phenolic hydroxyl groups might play important roles in the curcumin's anti-oxidant, anticancer activity and radicals scavenging,[50,51] indicating that

phenolic hydroxyl groups of the curcumin on the surface of the as-prepared cAgNPs might also play an important role in the antiviral activity. On the other hand, the absorption peak at 1627 cm^{-1} in curcumin, owing to a contemporaneous contribution of C=C and C=O stretching mode, shifted to 1635 cm^{-1} in cAgNPs, while the strong absorption peaks at 1149 cm^{-1} and 1276 cm^{-1}, which assigned to the enol C-O peak of pure curcumin, disappeared in cAgNPs, but appeared at 1381 cm^{-1} probably due to the binding of Ag with the C=O group of the curcumin. The FTIR data showed that the as-prepared AgNPs was capped with curcumin successfully and functioned with the C=O group.

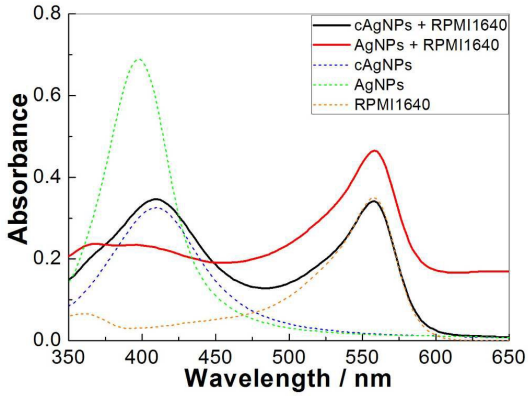

Figure 3. Comparison of the stability of the cAgNPs and the AgNPs capped with citric acid in RPMI 1640 (RPMI 1640 was used in the RSV adsorption steps).

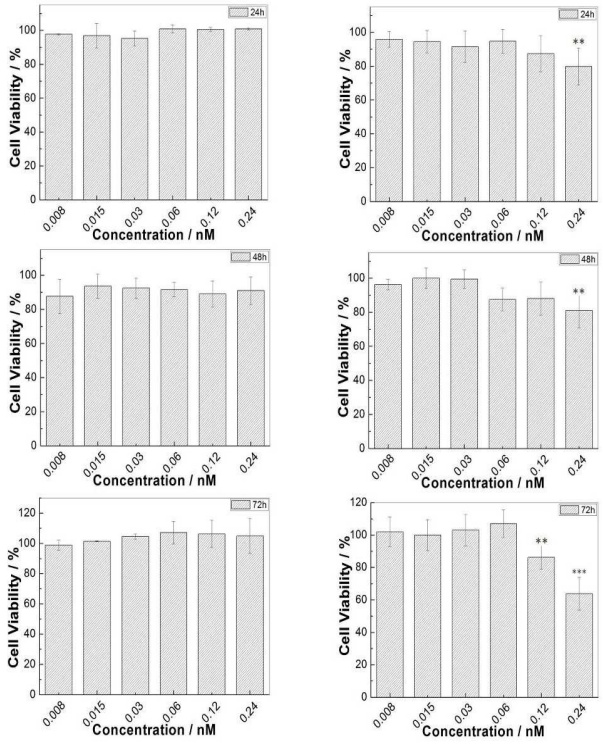

Figure 4. Biocompatibility of cAgNPs (the left column) and AgNPs capped with citrate acid (the right column) with Hep-2 cells. Hep-2 cells were exposed to cAgNPs or AgNPs capped with citrate acid for 24, 48 and 72 hours. The concentration of cAgNPs and AgNPs capped with citric acid were 0.008, 0.015, 0.03, 0.06, 0.12, 0.24 nM. Each experiment performed in triplicate, the error bar represents the standard deviation, **P*<0.05 vs. control.

Stability and cytotoxicity test

To investigate the stability of cAgNPs in the biological environment and its toxicity, the ultraviolet spectrum was used for identifying the stability of cAgNPs in Hep-2 cell-culture medium (RPMI 1640) and the CCK-8 cell viability assay was used to investigate the cytotoxicity of cAgNPs *in vitro*. Figure 3 showed that the cAgNPs have benign solubility and stability in the cell culture medium (RPMI 1640). By contrast, the conventional silver nanoparticles capping with citric acid are unstable and quite easy to aggregate in the RPMI 1640 solutions, and the characteristic absorption peak of AgNPs at 400 nm gets disappeared.

Figure 4 showed that the cAgNPs had very low toxicity since the cell viability was more than 95% at all test conditions (Figure 4, the left column). The AgNPs obtained with citric acid, however, showed apparent cytotoxicity with cell co-incubation for 72 h when its concentration was 0.12 nM and 0.24 nM (Figure 4, the right column). That is to say, the non-toxic concentrations of AgNPs obtained with citric acid to Hep-2 cells are far less than that of cAgNPs, indicating that our newly prepared cAgNPs are safer and more stable than the AgNPs capped with citric acid in biological environment. The curcumin alone also showed low toxicity to Hep-2 cells (Figure S1).

Interaction of cAgNPs with RSV

The interaction between nanoparticles and virus mainly include inactivating the virus directly, blocking viral entry into the cells, and interfering the viral replication and budding.[4,8,12,15,23,52] Each stage of virus infection maybe a possible target for inhibition. To understand the antiviral mechanism of cAgNPs involved in RSV, it should at first identify whether or not there are direct

Table 2. DLS measurements of nanoparticles in solution

	Size ± SD (nm)
cAgNPs	13.69 ± 0.05
RSV	122.90 ± 3.53
cAgNPs + RSV	193.57 ± 14.85

DLS measurements of cAgNPs and virus alone, cAgNPs incubated with RSV for 1 hour with average size.

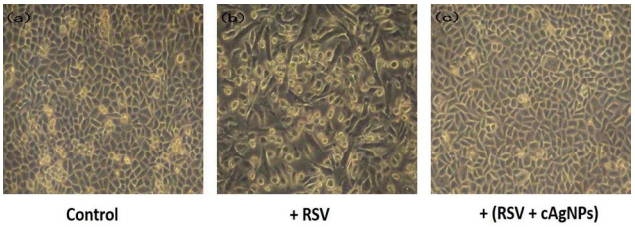

Figure 5. The cytopathic effect (CPE) result of Hep-2 cells infected with untreated and cAgNPs treated RSV. The mock Hep-2 cells (a) exhibit no CPE. Obvious CPE is observed in the group of the Hep-2 cells infected with RSV (b). The Hep-2 cells infected with cAgNPs inactivating RSV (c) (cAgNPs incubated with RSV for 1 h prior to infect Hep-2 cells) show rarely CPE (The virions and cAgNPs were removed after viral adsorption).

interactions between cAgNPs and RSV. The dynamic light scattering (DLS) measurements (Table 2) showed that the mean size of cAgNPs pre-treated RSV was about 200 nm, which was much larger than cAgNPs and RSV alone. The possible reason might be the direct attachment of cAgNPs to the viral envelop grycoproteins.

In such case, we can suppose that the infectivity of RSV would get reduced if RSV at first interacting with cAgNPs. In order to identify that, photo images of cytopathic effect (CPE) were investigated to observe the impact on virus infectivity. As Figure 5 showed, no CPE was found in the control group (Figure 5a), but obvious syncytia formation was observed and some infected cells began to die in the group of Hep-2 cells infected with RSV alone (Figure 5b). If RSV was pre-treated with cAgNPs for 1 h prior to infection, however, significant CPE was scarcely found (Figure 5c). These results suggested that cAgNPs interacted with the viral envelope glycoproteins directly and interfered with the infectivity of RSV. This comparison also indicated that the viral titers of RSV might be decreased.

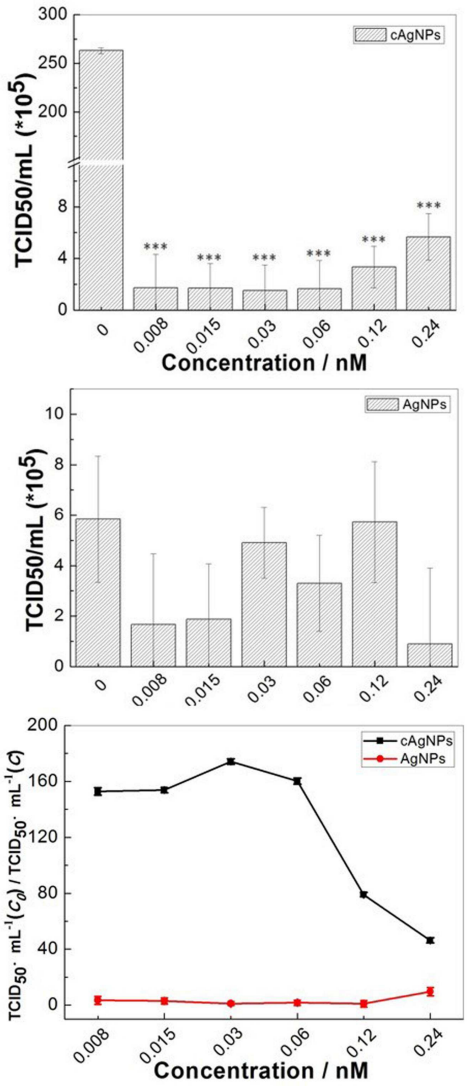

Figure 6. Antiviral properties of curcumin-AgNPs (cAgNPs) and AgNPs capped with citric acid (obtained with conventional method). The viral titers of RSV pre-treated with cAgNPs (a); The viral titers of RSV pre-treated with AgNPs capped with citric acid (b); the comparison of the two kinds AgNPs antiviral ability (c). $TCID_{50}{\cdot}mL^{-1}(C_0)$ stands for the viral titers of RSV without nanoparticles; $TCID_{50}{\cdot}mL^{-1}(C)$ stands for the viral titers of RSV pre-treated with nanoparticles, C is the concentration of nanoparticles correspondingly.

Antiviral activity of cAgNPs against RSV infection

The reduction of the viral titers of RSV could be further identified by $TCID_{50}$ assay, and the change of the viral titers of RSV after treating with different concentration of cAgNPs could be quantitatively measured. Figure 6a showed the viral titers of RSV pre-treated with cAgNPs. The viral titers of RSV were decreased significantly because cAgNPs might attach to the virions and inactivate RSV directly. For comparison, the ability of AgNPs capped with citric acid (synthesized with conventional method) to inactivate RSV was examined under the same experimental conditions (Figure 6b). Both cAgNPs and AgNPs capped with citric acid had a significant reduction in viral titers, but the reduction of the viral titers of RSV pre-treated with cAgNPs was much better (Figure 6c). It was found that the cAgNPs could decrease two orders of magnitude in viral titers, whereas the AgNPs only gets decreased one order of magnitude in viral titers to the greatest extent. In order to highlight the advantages of cAgNPs, we investigated the antiviral activity of curcumin (Figure S2 and Table S1). The reduction of the viral titers causing by curcumin was not as much as that causing by cAgNPs. From these results, we could conclude that the antiviral activity of cAgNPs was better than that of AgNPs capped with citric acid and that of curcumin. This might be owing to the benign properties both of AgNPs and curcumin. So the cAgNPs might be an excellent virus inactivating agent against RSV infection.

To establish the multifunctional usage of cAgNPs during the different stages of RSV infection, other different treatments were used for the addition of cAgNPs to Hep-2 cells: (1) incubation with cells for 1 h before RSV infection (cell pre-treatment assay), (2) after virus adsorption for 1 h (cell post-treatment assay). As Figure S3 showed, the viral titers of the harvest virus decreased to some extent both in the cell pre-treatment assay and in the cell post-treatment assay. These findings might illustrate that cAgNPs could prevent the virus from entering into cells and its replication to some extent.

The above results imply that cAgNPs indeed possess efficient antiviral activity against RSV infection. From the present study it was observed that cAgNPs significantly inhibited RSV infection by inactivating RSV directly prior to entry into the cells. Moreover, cAgNPs were able to reduce virus infectivity when added before RSV infection or after RSV infection to some extent. But the reduction in viral titers of cell pre-treatment assay and cell post-treatment assay were not as effective as that of virus pre-treatment assay. This showed that the main antiviral activity of cAgNPs was the direct inactivation of RSV.

Plaque assay

The plaque assay was taken to further identify the inhibition effects of cAgNPs against RSV. From the results (Figure 7), we

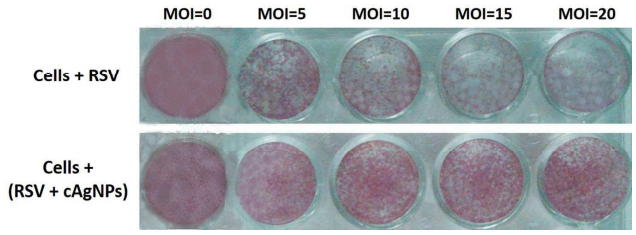

Figure 7. Plaque-reduction assay using Hep-2 cells infected with different MOI of RSV. The first column showed the Hep-2 cells infected by RSV. The second column was that RSV interacted with cAgNPs at 4 °C for an hour prior to infect the Hep-2 cells.

could observe that the plaque quantity increased significantly with increasing the MOI of RSV. By contrast, the plaque quantity of the group which RSV was interacting with cAgNPs prior to infect Hep-2 cells were obviously less than the group that infecting with RSV only under the same experimental conditions. In the control group, there was no plaque appeared at the well of cells without RSV. The pictures showed that the cAgNPs had benign antiviral activity to RSV intuitively.

Immunofluorescence assay of cAgNPs-RSV interaction

Indirect immunofluorescence assay with virus antibody was proved to be a very useful diagnostic technique.[53] Monoclonal antibody specific to G protein of RSV and Dylight 488-labeled goat anti-mouse IgG were employed herein to observe the interaction between cAgNPs and RSV through fluorescent microscopy. As Figure 8 showed, the nucleus were stained with Hoechst 33258 (blue) and the RSV G proteins were marked with green color. The control did not have any green fluorescence (the first row in Figure 8), while Hep-2 cells infected by RSV only

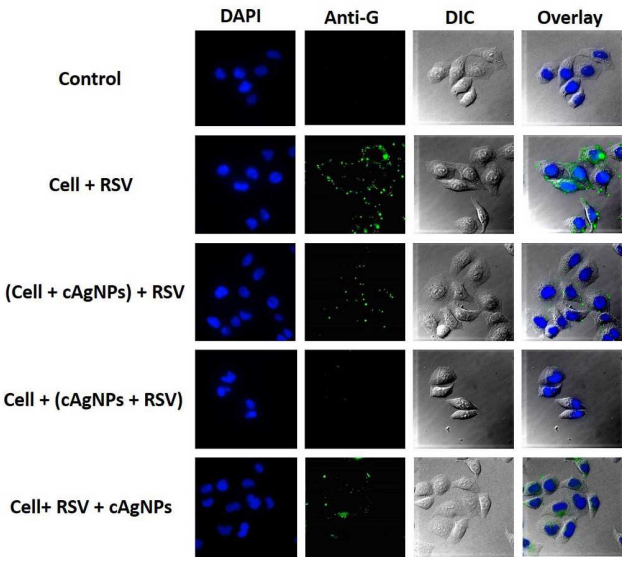

Figure 8. The inhibition effects of cAgNPs against RSV by immunofluorescence staining (60× oil immersion objective). The first row showed the Hep-2 cells only, and the second row showed the Hep-2 cells infected by RSV. The third row was that the Hep-2 cells pre-incubated with cAgNPs for 1 h before RSV infection. The fourth row was that RSV interacted with cAgNPs for 1 h prior to infect the Hep-2 cells. The fifth row was that Hep-2 cells co-incubated with RSV and cAgNPs.

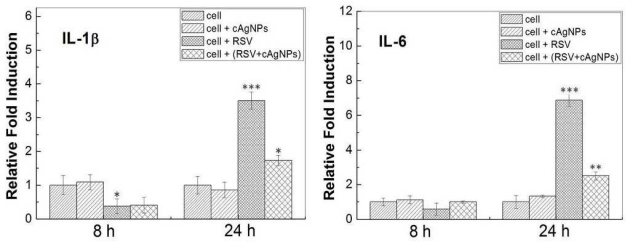

Figure 9. The mRNA expressions of IL-1β and IL-6 in Hep-2 cells after RSV infection with or without cAgNPs. Hep-2 cells were incubated with RSV or cAgNPs pre-treated RSV, and cells were harvested at 8 and 24 h after infection for total RNA extraction. Untreated cells as control and β-actin served as an internal reference. Date were expressed as mean ± SD (n=3).

had obvious green fluorescence around the cell membrane (the second row in Figure 8). When Hep-2 cells pre-treated with cAgNPs before RSV infection, the green fluorescence could be observed. But the fluorescence intensity was slightly weaker than that in the RSV-infecting group (the third row in Figure 8), indicating that cAgNPs could only prevent RSV from adsorbing to cells to a small extent. This result was consistent with the outcome of the viral titers assay (Figure S3). The green fluorescence could not be observed for those Hep-2 cells infected with cAgNPs pre-treated RSV (the fourth row in Figure 8). When the Hep-2 cells were infected with RSV in the presence of cAgNPs, the green fluorescence was weaker than that in the RSV-infected group (the fifth row in Figure 8), indicating that cAgNPs could block the viral attachment. These results further demonstrate the efficient antiviral activity of cAgNPs against RSV infection. And we concluded that the cAgNPs played an effective role in inactivating RSV prior to entry into the cells. Meanwhile, the cAgNPs could block RSV attachment and prevent RSV from infecting cells to a small extent.

Gene expression assay of cAgNPs-RSV interaction

IL-1β and IL-6 are important cytokines which could be detected in RSV-infected respiratory epithelial cell cultures in vitro.[53] To further examine the inhibition of cAgNPs against the RSV, we screened the gene expression of IL-1β and IL-6 using real-time quantitative PCR in RSV infected Hep-2 cells with or without cAgNPs. As shown in Figure 9, the gene expression levels of IL-1β and IL-6 were lower than the control group at the early stage of RSV infection, while the levels of IL-1β and IL-6 both got increased significantly at 24 h after infection with RSV. In Hep-2 cells infected with RSV without cAgNPs, extremely significant upregulation of IL-1β and IL-6 was observed compared to the control group. While in Hep-2 cells infected with RSV pre-treated by cAgNPs, downregulation of IL-1β and IL-6 was observed compared to the cells with RSV infection only, indicating that cAgNPs pre-treated RSV could decrease the cells responses to RSV infection. At the same time, no significant difference of the expression of these cytokines was observed in the group of Hep-2 cells treated with cAgNPs only. These results

indicated that the cAgNPs really possess significant anti-RSV activity.

Conclusions

In conclusion, we investigated that silver nanoparticles functionalized by curcumin have remarkable antiviral activity against RSV infection for the first time. The cAgNPs were uniform, stable, mono-dispersed, and had fine bioavailability. The cAgNPs could reduce CPE induced by RSV and showed efficient antiviral activity against RSV infection by directly inactivating the virus prior to entry into the host cells. Moreover, cAgNPs exhibited antiviral activity when incubated before, simultaneously or after with the onset of viral infection to some extent. Compared with the conventional silver nanoparticles capped with citric acid, the cAgNPs were more stable in physiological environment and possessed better antiviral properties. More pharmacodynamics and toxicological studies of cAgNPs in appropriate animal models would be needed in future investigations. According to our results, curcumin-AgNPs might be potential to be developed as a promising virucide for RSV.

Acknowledgements

This work was financially supported by the National Natural Science Foundation of China (NSFC, 21535006) and the Postdoctoral Science Foundation of Chongqing (No. xm2014001).

Notes and references

Key Laboratory on Luminescence and Real-Time Analytical Chemistry (Southwest University), Ministry of Education, College of Pharmaceutical Science, Southwest University, Chongqing 400715, China. E-mail: chengzhi@swu.edu.cn; Fax: +86 23 68367257; Tel: +86 23 68254659

1. P. K. Jain, X. Huang, I. H. El-Sayed and M. A. El-Sayed, *Acc. Chem. Res.*, 2008, **41**, 1578-1586.
2. N. Sanvicens and M. P. Marco, *Trends Biotechnol.*, 2008, **26**, 425-433.
3. I. Papp, C. Sieben, K. Ludwig, M. Roskamp, C. Böttcher, S. Schlecht, A. Herrmann and R. Haag, *Small*, 2010, **6**, 2900-2906.
4. D. Baram-Pinto, S. Shukla, A. Gedanken and R. Sarid, *Small*, 2010, **6**, 1044-1050.
5. B. M. DeRussy, M. A. Aylward, Z. Fan, P. C. Ray and R. Tandon, *Sci. Rep.*, 2014, **4** 5550.
6. M. Sametband, S. Shukla, T. Meningher, S. Hirsh, E. Mendelson, R. Sarid, A. Gedanken and M. Mandelboim, *MedChemComm*, 2011, **2**, 421-423.
7. J. Vonnemann, C. Sieben, C. Wolff, K. Ludwig, C. Bottcher, A. Herrmann and R. Haag, *Nanoscale*, 2014, **6**, 2353-2360.
8. T. E. Antoine, Y. K. Mishra, J. Trigilio, V. Tiwari, R. Adelung and D. Shukla, *Antiviral Res.*, 2012, **96**, 363-375.
9. M. Sametband, I. Kalt, A. Gedanken and R. Sarid, *ACS Appl. Mater. Inter.*, 2013, **6**, 1228-1235.
10. J. J. Liang, J. C. Wei, Y. L. Lee, S. H. Hsu, J. J. Lin and Y. L. Lin, *J. Virol.* , 2014, **88**, 4218.
11. L. A. Osminkina, V. Y. Timoshenko, I. P. Shilovsky, G. V. Kornilaeva, S. N. Shevchenko, M. B. Gongalsky, K. P. Tamarov, S. S. Abramchuk, V. N. Nikiforov, M. R. Khaitov and E. V. Karamov, *J. Nanopart. Res.*, 2014, **16**, 2430.
12. S. Galdiero, A. Falanga, M. Vitiello, M. Cantisani, V. Marra and M. Galdiero, *Molecules*, 2011, **16**, 8894-8918.
13. N. Wang, BoHu, M.-L. Chen and J.-H. Wang, *Nanotechnology*, 2015, **26**, 195703-195711
14. J. L. Elechiguerra, J. L. Burt, J. R. Morones, A. Camacho-Bragado, X. Gao, H. H. Lara and M. J. Yacaman, *J. Nanobiotech.*, 2005, **3**, 6-16.
15. H. H. Lara, N. V. Ayala-Nunez, L. Ixtepan-Turrent and C. Rodriguez-Padilla, *J. Nanobiotech.* , 2010, **8**, 1.
16. D. K. Singh and H. t. H. Lara, *Retrovirology*, 2012, **9**, O1.
17. D. Xiang, Q. Chen, L. Pang and C. Zheng, *J. Virol. Methods*, 2011, **178**, 137-142.
18. Y. Mori, T. Ono, Y. Miyahira, V. Q. Nguyen, T. Matsui and M. Ishihara, *Nanoscale Res. Lett.*, 2013, **8**, 93.
19. J. V. Rogers, C. V. Parkinso, Y. W. Choi, J. L. Speshock and S. M. Hussain, *Nanoscale Res. Lett.*, 2008, **3**, 129-133.
20. N. Chen, Y. Zheng, J. Yin, X. Li and C. Zheng, *J. Virol. Methods* 2013, **193**, 470- 477.
21. J. L. Speshock, R. C. Murdock, L. K. Braydich-Stolle, A. M. Schrand and S. M. Hussain, *J. Nanobiotech.* , 2010, **8**, 19.
22. D. Baram-Pinto, S. Shukla, N. Perkas, A. Gedanken and R. Sarid, *Bioconjugate Chem.* , 2009, **20**, 1497-1502.
23. P. Orlowski, E. Tomaszewska, M. Gniadek, P. Baska, J. Nowakowska, J. Sokolowska, Z. Nowak, M. Donten, G. Celichowski, J. Grobelny and M. Krzyzowska, *Plos one*, 2014, **9**, e104113.
24. L. Lu, R. W. Y. Sun, R. Chen, C. K. Hui, C. M. Ho, J. M. Luk, G. K. K. Lau and C. M. Che, *Antivir Ther*, 2008, **13**, 253-262.
25. N. Khandelwal, G. Kaur, N. Kumar and A. Tiwari, *Digest Journal of Nanomaterials and Biostructures* 2014, **9**, 175 - 186.
26. W. Wu, J. Shen, P. Banerjee and S. Zhou, *Biomaterials* 2011, **32**, 598e609.
27. K. I. Priyadarsini, *J. Photochem. Photobio. C:Photochemistry Reviews*, 2009, **10**, 81-95.
28. Bhawana, R. K. Basniwal, H. S. Buttar, V. K. Jain and N. Jain, *J. Agric. Food Chem.*, 2011, **59**, 2056-2061.
29. D. K. Singh, R. Jagannathan, P. Khandelwal, P. M. Abraham and P. Poddar, *Nanoscale*, 2013, **5**, 1882-1893.
30. K. Obata, T. Kojima, T. Masaki, T. Okabayashi, S. Yokota, S. Hirakawa, K. Nomura, A. Takasawa, M. Murata, S. Tanaka, J. Fuchimoto, N. Fujii, H. Tsutsumi, T. Himi and N. Sawada, *Plos one*, 2013, **8**, 70225-70239.
31. P. Anand, A. B. Kunnumakkara, R. A. Newman and B. B. Aggarwal, *Mol. Pharm.*, 2007, **4**, 807-818.
32. M. Donalisio, M. Rusnati, V. Cagno, A. Civra, A. Bugatti, A. Giuliani, G. Pirri, M. Volante, M. Papotti, S. Landolfo and D. Lembo, *Antimicrob. Agents Ch.* , 2012, **56**, 5278-5288.
33. S. Krishnan, M. Halonen and S. R. Robert C. Welliver, *Viral Immunol.*, 2004, **17**, 220-233.
34. S. S. Bawage, P. M. Tiwari, S. Pillai, V. Dennis and S. R. Singh, *Advances in Virolog*, 2013.
35. W. Zhang, E. Moore and R. A. Tripp, *Future Microbiol.* , 2009, **4**, 279-297.
36. M. T. Lotz and R. S. P. l. Jr, *Curr. Allergy. Asthma. Rep.*, 2012, **12**, 380- 387.
37. S. M. Bueno, P. A. González, C. A. Riedel, L. J. Carreno, A. E. Vásquez and A. M. Kalergis, *Immunol. Lett.*, 2011, **136**, 122-129.
38. J. Harris and D. Werling, *Cellular Microbiology*, 2003, **5**, 671-680.
39. L. L. Zheng, X. X. Yang, Y. Liu, X. Y. Wan, W. B. Wu, T. T. Wang, Q. Wang, S. J. Zhen and C. Z. Huang, *Chem. Commun.*, 2014, **50**, 15776-15779
40. L. Zhan, W. B. Wu, X. X. Yang and C. Z. Huang, *New Journal of Chemistry*, 2014, **38**, 2935-2940.
41. L. Zhan, C. M. Li, W. B. Wu and C. Z. Huang, *Chem. Commun.*, 2014, **50**, 11526-11528.
42. W. Wang, L. Zhan, Y. Q. Du, F. Leng, Y. Chang, M. X. Gao and C. Z. Huang, *Anal. Methods*, 2013, **5**, 5555-5559.
43. Y. Q. Du, P. F. Gao, W. Wang, T. T. Wang, Y. Chang, J. Wang and C. Z. Huang, *Analyst*, 2013, **138**, 5745-5750.
44. X. Y. Wan, L. L. Zheng, P. F. Gao, X. X. Yang, C. M. Li, Y. F. Li and C. Z. Huang, *Sci. Rep.*, 2014, **4**, 4529.
45. L. Sun, A. K. Singh, K. Vig, S. R. Pillai and S. R. Singh, *J.*

Biomed. Nanotechnol. , 2008, **4**, 149-158.
46. C. M. Li, L. L. Zheng, X. X. Yang, X. Y. Wan, W. B. Wu, S. J. Zhen, Y. F. Li, L. F. Luo and C. Z. Huang, *Biomaterials*, 2016, **77**, 216-226.
47. D. Steinigeweg and S. Schlücker, *Chem. Commun.*, 2012, **48**, 8682-8684.
48. L. Wei, J. Lu, H. Xu, A. Patel, Z. Chen and G. Chen, *Drug Discovery Today*, 2015, **20**, 595-601.
49. M. Murphy, K. Ting, X. Zhang, C. Soo and Z. Zheng, *J. Nanomater.*, 2014, **2015**.
50. K. K. Soudamini and R. Kuttan, *J. Ethnopharmacol.*, 1989, **27**, 227-233.
51. J. R. Fuchs, B. Pandit, D. Bhasin, J. P. Etter, N. Regan, D. Abdelhamid, C. Li, J. Lin and P.-K. Li, *Bioorg. Med. Chem. Lett.*, 2009, **19**, 2065-2069.
52. J. Trigilio, T. E. Antoine, I. Paulowicz, Y. K. Mishra, R. Adelung and D. Shukla, *Plos one*, 2012, **7**, e48147.
53. X. Lv, P. Wang, R. Bai, Y. Cong, S. Suo, X. Ren and C. Chen, *Biomaterials* 2014, **35**, 4195-4203.